Construction and Building Materials 411 (2024) 134069

Contents lists available at ScienceDirect

Construction and Building Materials

journal homepage: www.elsevier.com/locate/conbuildmat

# High-performance timber-concrete-composites with polymer concrete and beech wood

Sandro Stucki [a,b], Steffen Kelch [c], Tim Mamie [c], Urs Burckhardt [c], Philippe Grönquist [d,e,f], Roman Elsener [b], Mark Schubert [b], Andrea Frangi [f], Ingo Burgert [a,b,*]

[a] Wood Materials Science, Institute for Building Materials, Laura-Hezner-Weg 7, ETH Zürich, 8093 Zürich, Switzerland
[b] Cellulose & Wood Materials Laboratory, Empa, Überlandstrasse 129, 8600 Dübendorf, Switzerland
[c] Sika Technology AG, Tüffenwies 16, 8048 Zürich, Switzerland
[d] Institute of Construction Materials, University of Stuttgart, Pfaffenwaldring 4b, 70569 Stuttgart, Germany
[e] Materials Testing Institute, University of Stuttgart, Pfaffenwaldring 4b, 70569 Stuttgart, Germany
[f] Timber Structures, Institute of Structural Engineering, Stefano-Franscini-Platz 5, ETH Zürich, 8093 Zürich, Switzerland

ARTICLE INFO

*Keywords:*
Polymer concrete
Beech wood
Adhesion
Moisture stability
Timber-concrete composites
Bondline characterization

ABSTRACT

The performance of adhesive-bonded timber-concrete-composites (TCC) can be enhanced by using beech wood and polymer concrete (PC). In this work, two different PCs with an epoxy- and a polyurethane (PUR)-based matrix were investigated for application in TCCs. The mechanical performances were tested in dry and wet state by small-scale shear tests and flexural tests. Epoxy-PC showed high bond strength to beech with a shear strength of 16.7 ± 3.0 MPa compared to 3.2 ± 1.7 MPa observed with PUR-PC. Characterization of the swelling strain with digital image correlation (DIC) showed superior water stability of the epoxy-PC compared to PUR-PC. The results indicate that PCs, especially epoxy-PC, could be viable replacements for cement-based concrete in TCCs.

## 1. Introduction

Timber-concrete composites (TCCs) have been successfully introduced in the construction of bridges or medium to long-span floor systems [1]. While mostly mechanical connectors (nails, screws, etc.) or notches have been used to achieve the required shear stress transfer between the concrete and the timber layers, more recently, there is an increasing interest in replacing mechanical connectors with adhesively-bonded structures [2–15]. An advantage of using adhesive as a connector is a stiff connection with homogeneously distributed shear transfer across the layers. This allows to fully exploit the composite action of both, the concrete in the compression zone and the timber in the tension zone.

Previous research showed that in adhesive-bonded TCC with ordinary Portland cement (OPC), besides bending failure in the timber [12,14,16], compression failure in the concrete is an often-observed failure mode [11,17,18]. To overcome the strength limits of OPC used in TCC and to increase the strength of the TCC by avoiding concrete failure, polymer concretes (PC) pose a promising alternative to the commonly used OPC-based concretes. PCs are water-free systems, where the cement hydrate binders of conventional concrete are fully replaced by thermoplastic polymer binders or liquid resins, and the aggregates of the filler material are strongly bound to each other by the polymeric binders [19,20]. Depending on the selected resin matrix, PCs exhibit significantly higher compression, tensile and shear strengths compared to OPC-based steel-reinforced concrete and the strong self-adhesion of the PC to wood makes the application of additional adhesive unnecessary [9]. Successful applications of PCs in TCC have been shown by Erler [21] as well as Schober [9] by using PC in the compression zone. While Schober only tested epoxy-based concretes, Erler [21] additionally tested a polyester-based matrix. Shear tests showed that the adhesion and bulk strength of the PC to spruce wood exceeded the strength of spruce in most cases, resulting mainly in wood failure with neglectable concrete failure [9,21].

To further exploit the enhanced load-bearing capacity by the utilization of PC, an alternative approach is to apply beech wood in the tension zone of the TCC, rather than the conventionally used spruce.

Clear beech wood possesses on average superior mechanical properties (e.g. stiffness and strength) than spruce and is abundantly available in European forests [22,23]. However, one well-known challenge of beech in timber engineering is its hygrothermal behaviour. Beech can exhibit high moisture-induced swelling over its whole hygroscopic

* Corresponding author at: Wood Materials Science, Institute for Building Materials, Laura-Hezner-Weg 7, ETH Zürich, 8093 Zürich, Switzerland.
*E-mail address:* iburgert@ethz.ch (I. Burgert).

https://doi.org/10.1016/j.conbuildmat.2023.134069
Received 17 July 2023; Received in revised form 9 October 2023; Accepted 2 November 2023
Available online 23 November 2023

range [23]. This low dimensional stability poses a severe challenge for adhesive bonding between beech and the dimensionally very stable PC. The mismatch in the dimensional stability of the two materials may impose high stresses on the bondline upon changing moisture conditions, resulting in accumulated damage and eventually leading to the failure of the bondline. Application of adhesion primers as a pre-treatment of the wood surface is a well-known technology to improve the moisture resistance of wood-to-wood bonding [24,25]. It has previously been shown, that adhesion primer may also be applied in TCCs made from epoxy-adhesive bonded beech with OPC, leading to an increased load-bearing capacity of the TCC in dry state [5,26]. Schober [9] used a 2C-epoxy primer in a PC-based TCC, but did not test unprimed samples for comparison. Moreover, the influence of an adhesion primer on the moisture stability of the bondline has not yet been analysed for TCCs with PC.

In this work, we investigated two different PCs with epoxy- and polyurethane (PUR)- based matrixes for their applicability in TCC in combination with beech wood. Physical and chemical interactions of the resin with the wood surface were characterized by contact angle measurements and differential scanning calorimetry. In order to investigate the mechanical properties and the short-term moisture stability of the TCC, the bond strength of the PC to beech wood was characterized on small-scale TCC specimens in compression shear and flexural tests in dry state and in wet state after exposure to moisture. In addition to the native wood surface, we further explored the effect of a pre-treatment of the beech surface with a commercially available adhesion primer on the moisture stability of the bondline in the TCC. For an in-depth characterization of the influence of moisture on the TCC, we employed digital image correlation (DIC) to study the deformation behaviour of the TCC during moisture-induced swelling of the wood. The in-situ monitoring of the local deformation of the bondline and interfacial area revealed the influence of the respective PC on the moisture stability and provides relevant information for a further optimization of TCC produced with PC.

## 2. Material & methods

### 2.1. Materials

#### 2.1.1. Wood

European beech wood (*Fagus sylvatica*) of Swiss origin with a wood moisture content of approx. 8 % was supplied by Fagus Suisse SA (Les Breuleux, Switzerland) as glued-laminated-timber (GLT) [27] with a strength class grading of GL40h. The GLT was made from rectangular lamellae with a cross-sectional area of 40 x 40 $mm^2$, bonded by a melamine-urea–formaldehyde adhesive (MUF). The GLT was received with a planed surface and used without additional treatment (e.g. planing or sanding) of the surface before bonding.

#### 2.1.2. Polymer concrete (PC)

**Epoxy-PC:** A commercially available 3-part polymer grout "Sikadur®-42 LE Plus" was used as epoxy-PC. The grout consists of an epoxy resin with an amine-based hardener and mineral filler "Sikadur® 514".

**PUR-PC:** A 2C-PUR resin "SikaBiresin® F 50" with mineral filler "Sikadur® 514 Plus" was used as PUR-PC. The resin contains an isocyanate-based resin with a polyol-based hardener.

All components for the PC were produced by Sika Schweiz AG (Zürich, Switzerland). Quartz gravel (rounded grain shapes, grain size of 2.0–3.2 mm) from Amberger Kaolinwerke Eduard Kick GmbH & Co. KG. (Hirschau, Germany) was used in the flexural test specimens. Wetting and dispersing additive "BYK- 9076″ was obtained from BYK-Chemie GmbH (Wesel, Germany).

#### 2.1.3. Primer

A water-based 2C epoxy primer ("Sika® Primer MR Fast") produced by Sika Schweiz AG (Zürich, Switzerland) was used.

### 2.2. Characterization of wood-PC interaction

#### 2.2.1. Differential scanning calorimetry

For the measurement of the glass transition temperature $T_g$, samples were taken either from the interface or the bulk of the same specimen. Measurements were conducted in duplicate, with specimens sampled from different manufacturing batches of the PCs. The glass transition temperature was determined by Modulated Differential Scanning Calorimetry (MDSC) using a DSC Q2000 (TA Instrument, USA) with Tzero® aluminium pans. The PC was heated to 120 °C for 2 min immediately before the measurement to erase the thermal history. A heating rate of 5 °C/min with a superimposed temperature modulation on the main heating ramp (amplitude of 3.18 °C in a period of 60 s) was used. The glass transition was analysed with the Universal Analysis 2000 (TA Instruments) software through the inflexion point method based on the change in the reversing heat flow signal [28].

#### 2.2.2. Contact angle measurements

Contact angles were measured with the static sessile drop method on an OCA 20 (Dataphysics Instruments) contact angle system. Droplets of 10 µl of freshly mixed resin were placed on the beech wood on the longitudinal-radial (LR) surface. Images were recorded perpendicular to the fibre direction and the contact angle was calculated by the provided SCA 20 software. Care was taken that measurements took place within 5–10 min of mixing the resins to minimize changes in viscosity prior and during the measurements. The primed samples were prepared as described in chapter 2.2.2. 6 specimens were measured per configuration.

### 2.3. Specimen preparation for mechanical characterization

#### 2.3.1. Tensile test specimens of pure resin

Tensile test specimens of the resin used in the PC were made according to DIN EN 527–3, with a dumb-bell shaped specimen (type 5) [29]. The resins were prepared as used in the PC, without the addition of filler material, with a weight ratio of resin to hardener of 3:1 and 2:1 for the epoxy- and the PUR resin, respectively. The samples were cured for at least 28 days at 20 °C/35 % RH before measurement.

#### 2.3.2. Small TCC specimens for compression shear tests

Beech wood GLT was cut into specimens of defect-free beech wood with the dimension of 50x40x30 $mm^3$ with 40 mm being the longitudinal direction. Each specimen contained two beech wood lamellas with random annual ring orientation. For primed specimens, the wood surface was pre-treated 20–24 h before specimen preparation. The primer ("MR Fast") was prepared by mixing the resin and hardener (weight ratio of 2:1). 150 $g/m^2$ primer was applied by brush to the wood surface and left to cure at 20 °C/35 % RH. The PCs were prepared according to the manufacturer's recommendation, as listed in Table 1. In short, resin and hardener were mixed with an overhead stirrer equipped with a helical mortar mixer paddle. The mineral filler material was slowly added and stirred until a homogenous mixture was obtained. The shear test specimens were produced by placing the wood blocks in a mould,

**Table 1**
Mixture formulation of the PCs in parts (per weight) for the different test setups.

| | Epoxy PC | | PUR PC | |
|---|---|---|---|---|
| | Compression shear test | Flexural test | Compression shear test | Flexural test |
| Resin | 3 | 3 | 2 | 1.8 |
| Hardener | 1 | 1 | 1 | 1 |
| Filler | 34 | 22.6 | 24 | 13.4 |
| Quartz sand | – | 11.3 | – | 6.7 |
| Water | – | – | – | 0.006 |
| BYK-9076 | – | – | – | 0.09 |

with the 50x40 mm surface facing upwards. The freshly prepared PC was then directly poured onto the wood surface, obtaining a final dimension of the specimens of 50 × 40 × (30 + 30) $mm^3$. The specimens were left to cure at 20 °C/35 % RH for at least 28 days before measurement.

The moisture stability was tested by immersing the fully cured samples in tap water at room temperature for 24 h. The samples were tested in wet state immediately after removal from the water.

#### 2.3.3. TCC specimens for four-point flexural tests

Defect-free beech beams with the dimensions of 1020x60x30 $mm^3$ were prepared and conditioned at 20 °C/35 % RH. Each beam contained two lamellae with random annual ring orientation. For the flexural test specimens, part of the PC filler material was replaced by quartz sand, in a weight ratio of 2:1, as shown in Table 1. The epoxy-PC was prepared the same way as described before. In terms of PUR-PC, the wetting and dispersive agent "BYK-9076″ (alkylammonium salt of a high molecular-weight copolymer) and water were additionally added to improve the flow property and to adjust the shrinking behaviour during curing, respectively. Water was added as a foaming agent to reduce the cure shrinkage of the PC. Water reacts with the isocyanate group of the resin and converts it to an amine group under the release of $CO_2$. The resin-to-hardener ratio was adjusted to accommodate for the change in reactive groups of the resin, as listed in Table 1. The freshly prepared PC was poured directly on the beam surface to obtain a layer thickness of 15 mm PC, adjusting a ratio of 2:1 for the timber to PC thickness as described in [30]. The final specimen dimensions were 1020 × 60 × (30 + 15) $mm^3$. The specimens were cured at 20 °C/35 % RH for at least 28 days before testing. To test the moisture stability, the fully cured specimens were placed in a humid climate (20 °C/95 % RH) for at least 50 days before measurement.

### 2.4. Mechanical characterization

#### 2.4.1. Tensile tests of pure resin

A Zwick/Roell Z010 Universal testing machine with a 10 kN load cell was used. The testing speed was 1 mm/min, and the deformation was measured using a clip-on extensometer. The elastic modulus was calculated according to DIN EN ISO 527-1 [31] as the slope of the linear regression in the stress–strain curve between 0.05 and 0.25 % strain. 5 specimens were measured per material and test conditions.

#### 2.4.2. Compression shear tests of small TCC specimens

Compression shear strength was measured with a shear setup as shown in Fig. 1A. The specimens were supported at the backside to avoid tilting of the specimen, but minimal sideway movements were not restricted. Shear tests were conducted on a Zwick/Roell Z100 with a 100 kN load cell and a speed of test of 1 mm/min. The shear area was 50x40 mm and the load was applied in the fibre direction. The number of tested specimens per configuration is reported in Chapter 3.3 and Table S1.

#### 2.4.3. Four-point flexural tests on TCC specimens

The four-point flexural tests were conducted with a support span of 900 mm and a loading span of the test heads of 180 mm. The setup used is shown in Fig. 1B. A Zwick/Roell Z100 universal testing machine with a 100 kN load cell with a test speed of 5 mm/min was used, leading to failure within 100–450 s. The mid-span displacement was measured using a 2D-DIC-system (Q-400, Dante Dynamics) with software control (Istra 4D, Dante Dynamics). The flexural stiffness was calculated according to DIN EN 52186 [32] from the measured force–displacement curve between 10 and 40 % of the maximal force. Three specimens were tested per TCC configuration. In addition to the TCCs beams, pure beech wood GLT beams with beam heights of 30 and 60 mm were measured. For beams with 30 mm, only the elastic modulus was determined, whereas eight specimens of the 60 mm beams were tested until failure.

The governing strengths of the subcomponents of the dry specimen were calculated using the γ-method as described in Eurocode 5, appendix B [33]. With a fully rigid connection of the TCC, the γ-factors can be assumed as $\gamma_1 = y_2 = 1$ [18,30]. The elastic modulus of the timber subcomponent was approximated as a constant value with 14.6 GPa and the material properties of the concrete were used according to Table 2.

**Table 2**
Mechanical properties of the used PCs and their pure resins.

| | Compression | | Tension | |
|---|---|---|---|---|
| | Strength [MPa] | Elastic modulus [GPa] | Strength [MPa] | Elastic modulus [GPa] |
| Epoxy-PC | 119.9 ± 0.5 [a)] | 30.5 ± 3.0 [b)] | – | – |
| Resin only [c)] | – | – | *50.8 ± 3.7* | *3.3 ± 0.2* |
| Resin only- wet [d)] | – | – | *39.7 ± 5.3* | *2.7 ± 0.6* |
| PUR-PC | 97.4 ± 2.1 [a)] | 28.0 ± 1.2 [b)] | – | – |
| Resin only [c)] | – | – | *34.9 ± 1.7* | *2.9 ± 0.2* |
| Resin only- wet [d)] | – | – | *30.0 ± 1.7* | *2.5 ± 0.2* |

a) Measured on cylinder test specimen (n = 3) by [30], according to SN EN 206.
b) Measured on cylinder test specimen (n = 3) by [30], according to SN EN 12390-13.
c) Formulation of the resin used in the compression shear tests. Measured according to DIN EN ISO 527 [31].
d) After immersion in cold water for 14 days.

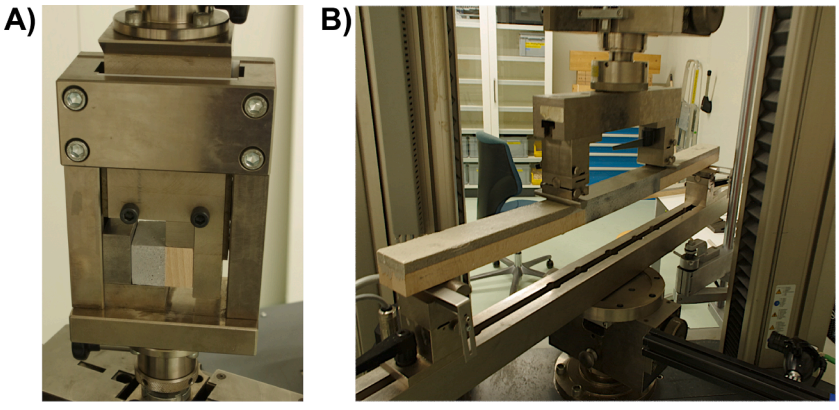


**Fig. 1.** Test setup for mechanical tests. A) Compression shear test, B) Four-point flexural test.

### 2.5. In-situ characterisation of the swelling strain with digital image correlation (DIC)

Millimeter-scale specimens were used for the in-situ characterisation of the swelling strain to achieve fast swelling and thus, to reduce the chance of mold growth during the measurement. Beechwood blocks with dimensions of approx. 25 × 30 × 10 $mm^3$ (T × R × L) were prepared and conditioned at 20 °C/35 % RH.

The PC was prepared as described in chapter 2.3.2 for the compression shear test specimens. The freshly prepared PC was poured on the longitudinal–tangential section of the woods, with at least 6 specimens per configuration. A black/white speckle pattern made with water-soluble acrylic resin was applied by a reagent sprayer on the sanded surface of the specimen. The speckles had a median area size of 6 pixels and an interquartile range (IQR) of 23 pixels. The specimens were conditioned at 20 °C/35 % RH and subsequently placed in a box modified with a see-through Plexiglas window equipped with a sample stand and a fan to ensure air circulation. The bottom of the box was filled with water to create a humid atmosphere (~90–95 % RH). Greyscale images with 6016 × 4000 pixels were taken of the sample with a K-3 II reflex camera (Pentax) equipped with an SP AF 90 mm F/2.8 Di Macro-Objective (Tamron). The pixel resolution was between 8.7 and 12.0 µm/px and was measured for each image by comparing specific landmarks in the recorded image (e.g. quartz grains) with images taken on a microscope (Olympus BX51) with calibrated magnification. The mean reprojection error of the images was 0.4 pixels, determined with the Matlab Single Camera Calibrator App [34].

The obtained images were post-processed with ImageJ [35]. The contrast of the speckle pattern was improved by histogram equalization to accommodate for different lighting conditions during the measurements [36]. If necessary, images were rotated to align the bondline horizontally in the image to ensure the subsequently calculated strains were oriented correctly regarding the bondline. Strains were calculated with the open-source DIC software "ncorr v1.2" [37] run on Matlab (R2020b, TheMathWorks, Inc., USA). The subset radius for DIC was chosen between 10 and 20 pixels and optimized for each image series. The strain radius was set as 5 pixels. The obtained 2D-strain matrix was exported as a false colour map for visualization. A subset of the obtained 2D-strain matrix was selected, where obvious defects (cracks in the wood, border effects, etc.) were excluded. This subset was then further reduced to a strain vector by averaging the strain row-wise and plotting the average strain and standard deviation thereof to obtain a 1D-strain curve as a function of the distance to the bondline.

## 3. Results & discussion

### 3.1. Wood-PC interaction

The interaction of the PC with the wood surface must be considered for the application of the PC in TCCs. An important property of adhesives is a good wetting of the wood surface by the resin, as it results in a high contact area between the wood and the resin and thus allows for a good stress transfer across the interface [38,39]. As seen in Fig. 2A, both resins (without the addition of filler) showed good wetting of the beech wood surface with a low contact angle in the range of 20°, independently of the application of an adhesion primer. The contact angles are in the same range as found for other widely applied wood adhesives [40].

The curing behaviour of the resin may be influenced by extractives or water from the wood [38]. Especially PUR-resins containing isocyanate groups are well known to react with moisture from the wood [41,42]. To investigate the potential influence of the wood surface on the curing of the resins, glass transition temperatures $T_g$ of resins taken from the wood-PC interface and the bulk of the PC were compared (Fig. 2B). In order to ensure no effect of minor variations in the mixing ratio of the components, the samples were taken from specimens produced in the same batch of PC. An influence of the wood on the curing of the resin can be seen by the spatial dependence of the $T_g$ in the PUR-PC. As determined by differential scanning calorimetry (DSC), the $T_g$ of the PUR-PC is about 14.6 °C lower at the interface than in the bulk, whereas no such difference in $T_g$ was observed with the epoxy-PC. Moisture from the wood reacts with the isocyanate of the PUR-PC and the resulting change in crosslink density may affect the physical properties of the cured PC [42]. It has to be noted, that this observation is only valid under the assumption that no demixing of the individual components of the PC occurs during the curing. However, demixing is not expected to be responsible for the spatial dependence of the $T_g$, since the application of an adhesion primer, producing a diffusion barrier for water vapour, showed a lower difference (5.6 °C) of the $T_g$ between the interface and bulk in the PUR-PC, as shown in Fig. 2B, thus indicating a protective effect of the adhesion primer against surface moisture.

### 3.2. Mechanical properties of the PC

Table 2 shows the mechanical properties of the investigated PCs and their resins. The epoxy-PC has a compression strength and elastic modulus comparable to ultra-high performance concrete (UHPC) [3] and about 2–3 times higher than OPC (e.g. C25/30, C30/37 [10,11]). The PUR-PC has about 20 % lower compression strength and 8 % lower

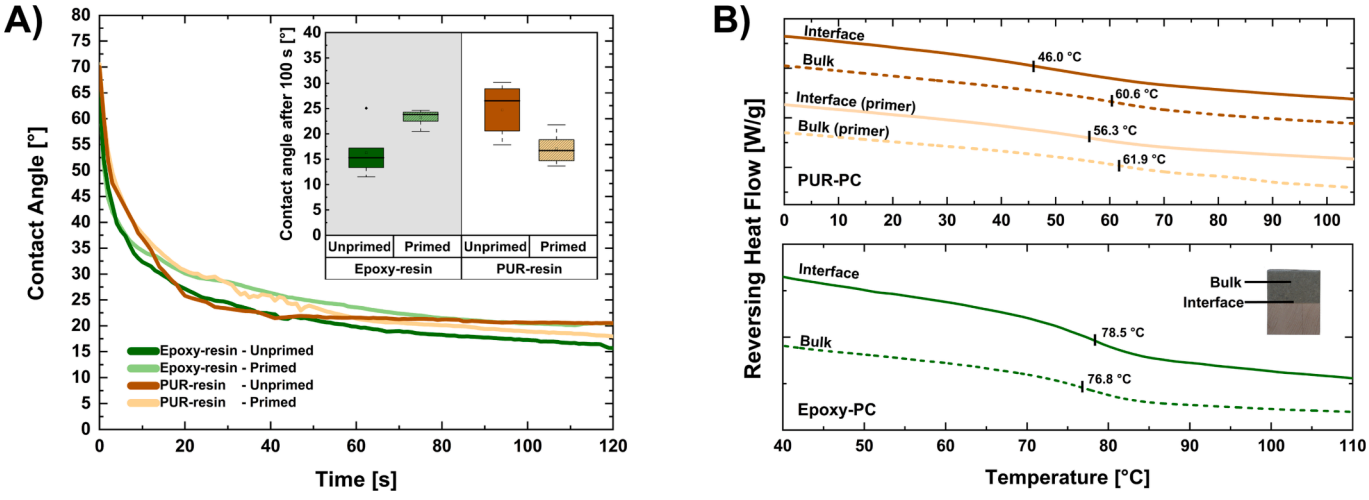


**Fig. 2.** Characterization of the resins used in the PC and their interaction with wood. A) Contact angle of the epoxy- and PUR-resins used in the formulation of the PC. B) DSC heat flow curves (exotherm up) with glass transition temperature Tg of the cured PUR-PC (top) and epoxy-PC (bottom).

elastic modulus than the epoxy-PC.

While the mineral fillers play an important role in compression, the resin plays a key part in tensile strength. Comparison of the unfilled, cured resin shows that the epoxy resin has approx. 30 % higher tensile strength and 12 % higher elastic modulus than the PUR resin.

Water influences the mechanical properties of the resins, as tested by immersion in tap water at room temperature for 14 days. The ultimate tensile strength of the resins is reduced by approx. 20 % (22 % and 18 % for the epoxy- and the PUR-resin, respectively) and the stiffness of both resins is about 14 % lower than in dry state.

### 3.3. Shear strength and moisture resistance of small TCC

#### 3.3.1. Shear performance of the bondline

An important characteristic of glued TCCs is the resulting adhesion strength between concrete and wood since an adequate shear strength is necessary to allow the stress transfer between the concrete and wood layers. The compression shear strengths of PC bonded to beech are shown in Fig. 3. TCC produced with epoxy-PC showed a high average shear strength of around 16.7 ± 3.0 MPa, with maximal values of up to 24.4 MPa. The bond strength exceeded the shear strength of the beech, resulting in a high proportion of wood failure (Fig. 4). Pre-treatment of the wood surface with an adhesion primer had no significant influence on the shear strength in dry state. In comparison, epoxy-PC with spruce, as tested by Schober [9], resulted in shear strengths of 6.16 MPa with wood failure in all the specimens. TCC produced with PUR-PC on the other hand showed lower shear strengths of 3.2 ± 1.7 MPa, which can be moderately increased to 5.2 ± 2.3 MPa through the application of an adhesion primer. Failure in the PUR-PC occurs mostly as near interface cohesion failure (c.f. Fig. 4C). The failure mostly didn't occur through the bulk of the concrete, but rather through the boundary layer between the bondline and the concrete bulk with a film of resin remaining on the wood surface. Such near interface cohesion failure shows that the resin has an adequate adhesion strength to the beech wood and that the shear strength is determined by the cohesion strength of the PUR- matrix near the interface.

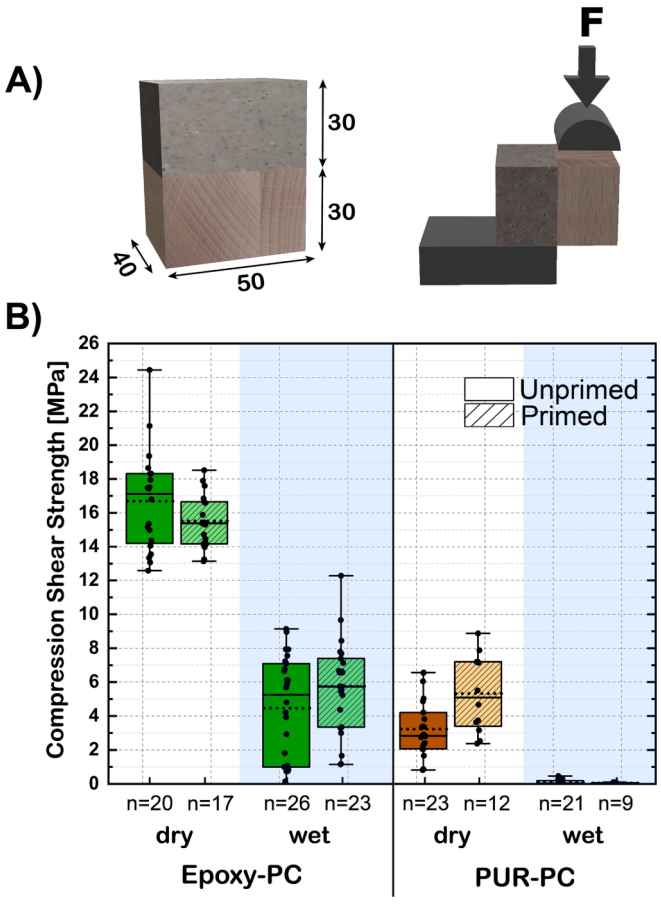


**Fig. 3.** A) Sample geometry and dimensions (in mm) and test setup B) Compression shear strength of TCC from beech wood with epoxy-PC and PUR-PC in dry state (conditioned at 35 % RH) and in wet state after 24 h water immersion. The box indicates the interquartile range with the median value marked by a solid line and the mean value by a dotted line.

#### 3.3.2. Influence of moisture

Moisture stability of TCC with glued interfaces has been recognized as a potential disadvantage of such systems, as the stiff connection of the two dissimilar materials may lead to high stresses at the interface due to moisture-induced swelling of the wood [2,10]. This effect is especially pronounced when using beech wood due to its low dimensional stability. There are no standard procedures to test the moisture stability of TCC, yet. However, to investigate the influence of moisture on the bond strength, we adapted a simplified water immersion test similar to treatment A2 of DIN EN 302–1. The immersion time of the samples in water was reduced to 24 h and the samples were tested in wet conditions. The sample geometry with its two different annual ring orientations led to a complex deformation behaviour of the wood part upon swelling, thus resulting in a mixture of shear and tensile forces acting on the bondline.

The observed compression shear strength decreased after water immersion of the specimens. Samples with PUR-PC showed a high proportion of premature failure during the water immersion, resulting in an average wet shear strength of 0.1 ± 0.1 MPa. Surprisingly, only a small amount of pure adhesion failure was detected and the majority of the samples failed as near interface cohesion failure (Fig. 4). This shows that the adherence of the PUR-PC resin to the wood still persisted even under wet conditions. Thus, the cohesive strength of the boundary layer between the interface and the bulk region of the PC, rather than the PC-wood interface, determined the shear strength.

While TCC bonded with epoxy-PC showed a high proportion of wood failure in dry state, the prevalent failure mode shifted to near interface cohesion failure after water immersion. Nonetheless, the epoxy-PC retained a shear strength of 4.5 ± 3.1 MPa in wet state and showed only a low amount of premature failure during the water immersion. The use of an adhesion primer had no significant effect on the wet shear strength for the investigated PCs. Additional images of the fracture surface of the epoxy-PC and PUR-PC can be found in Fig. S1 and S2, respectively.

### 3.4. Flexural tests of TCC- beams

#### 3.4.1. Flexural performance

The bending behaviour was investigated using four-point flexural tests on TCC with a thickness ratio of timber to concrete of 2:1, which was chosen to avoid tensile stresses in the concrete part and to maximize the timber content of the composite [30]. Fig. 5 and Table S2 show the flexural behaviour of the TCCs with PCs and pure beech wood GLTs. In flexural tests, the stiffness of beech wood GLT can be influenced by the beam height of the tested specimens [43]. Thus, two different GLT beam heights (30 and 60 mm) were tested to determine the range of flexural stiffness of the GLT (c.f. Table S3). While the beams of 30 mm height consisted of only one layer of lamellae, the beams of 60 mm height contained a horizontal bondline between two layers of beech wood lamellae. The beams with 60 mm height were tested until fracture to determine the strength and ensure that fracture does not occur in the horizontal bondline of the GLT between the beech wood lamellae. The stiffness of the GLT with 30 mm and 60 mm height resulted in a flexural modulus of 14.6 ± 2.5 GPa and 13.4 ± 0.4 GPa, respectively. Fig. 5C shows the strength and stiffness of the TCCs and the GLT beams with 60 mm height. Reinforcement of the beams with epoxy-PC led to an average

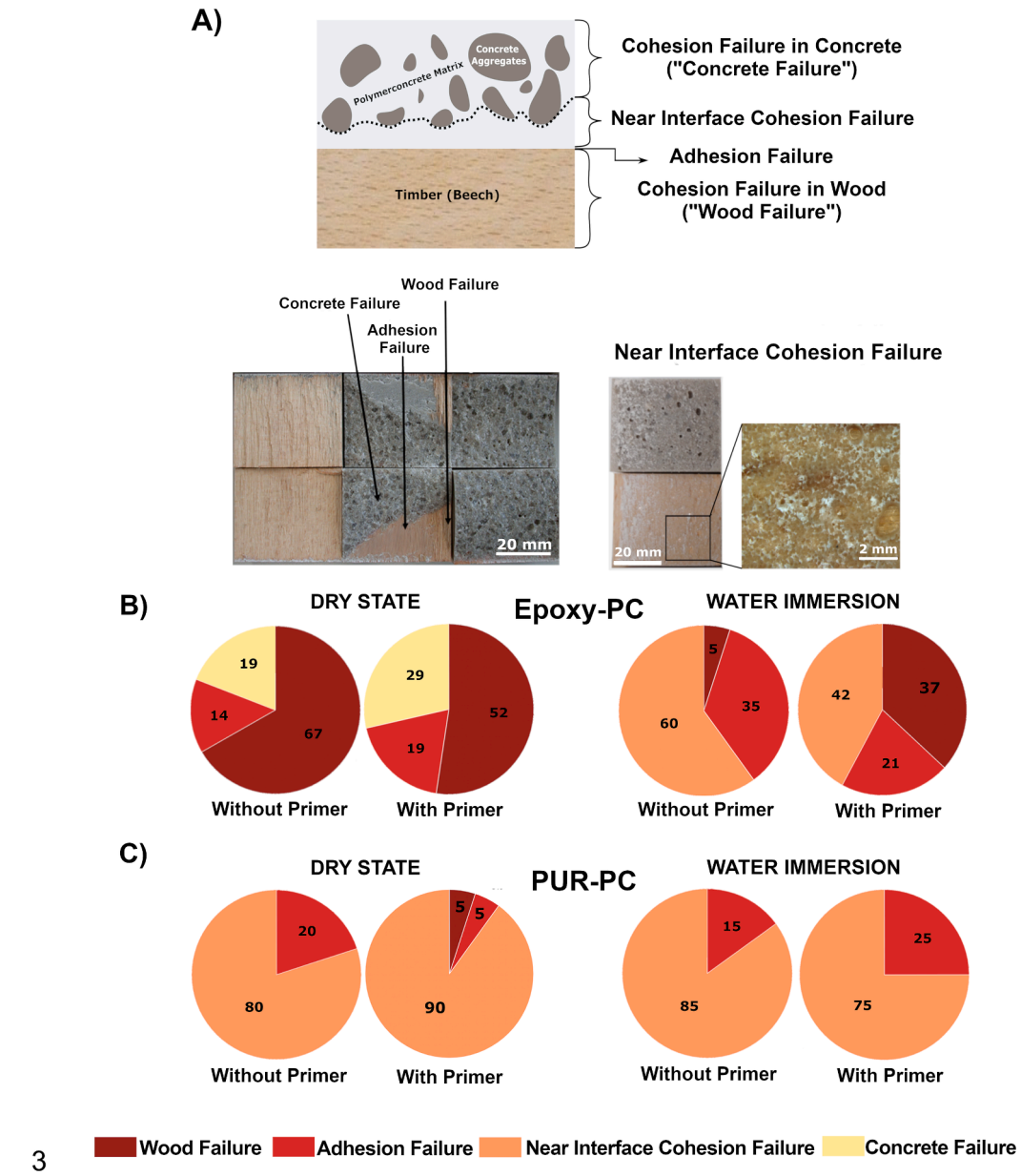


**Fig. 4.** Failure after shear tests of the TCC with A) Nomenclature used for the observed fractures and exemplary image of the fracture surfaces. Observed average fracture surfaces after compression shear test in dry and wet state of B) Epoxy-PC and C) PUR-PC. The shown values are the average of the fracture surface observed across all tested samples.

flexural modulus of 20.0 ± 1.8 GPa, thus showing the stiffening effect of the epoxy-PC reinforcement. PUR-PC in comparison did not significantly increase the stiffness of the beam with a mean flexural modulus of 15.5 ± 0.3 GPa.

The load-bearing capacity appeared to be improved by the reinforcement with epoxy-PC with a flexural strength of 131.3 ± 18.6 MPa for the TCC compared to 114.7 ± 11.6 MPa of pure beech GLT. However, this increase in strength was within the natural variability of beech wood, hence more samples would be required to characterize the strengthening effect of the epoxy-PC on the TCC. The PUR-PC on the other hand led to no increase in flexural strength compared to pure beech. Excluding the specimen with premature shear failure, PUR-PC reinforced beams show an average strength of 111.0 MPa.

### 3.4.2. *Failure modes*

The stresses acting on subcomponents of the TCC beams at the time of failure of the beams as calculated by composite theory [33] are shown in Table 3. The governing strength of the TCC with epoxy-PC is determined by the bending strength of the timber, with fracture starting from finger joints (if present) as shown in Fig. 5D and Fig. S3. Compression failure in the epoxy-PC was observed as secondary failure mode with visible cracks in the PC for two out of three specimens. The shear stresses acting on the bondline between GLT and PC at the time of failure were well below the shear strength of the bondline measured on the shear test sample. For the PUR-PC, the fracture was observed as near interface cohesion failure in shear, with comparable shear stresses as measured in the shear test specimens (Fig. 5D and Fig. S4). The shear failure occurred abruptly in all the PUR-PC specimens, with neither tensile-bending failure in the wood nor any obvious compression-induced cracks in the PC. This confirms that the governing strength of the TCC with PUR-PC is dictated by the interface region in the vicinity of the bondline between GLT and PC. A similar behaviour was observed by Grönquist et al. [30] in flexural tests on large-scale TCC beams (5.2 m) made of beech wood with epoxy- and PUR-PC.

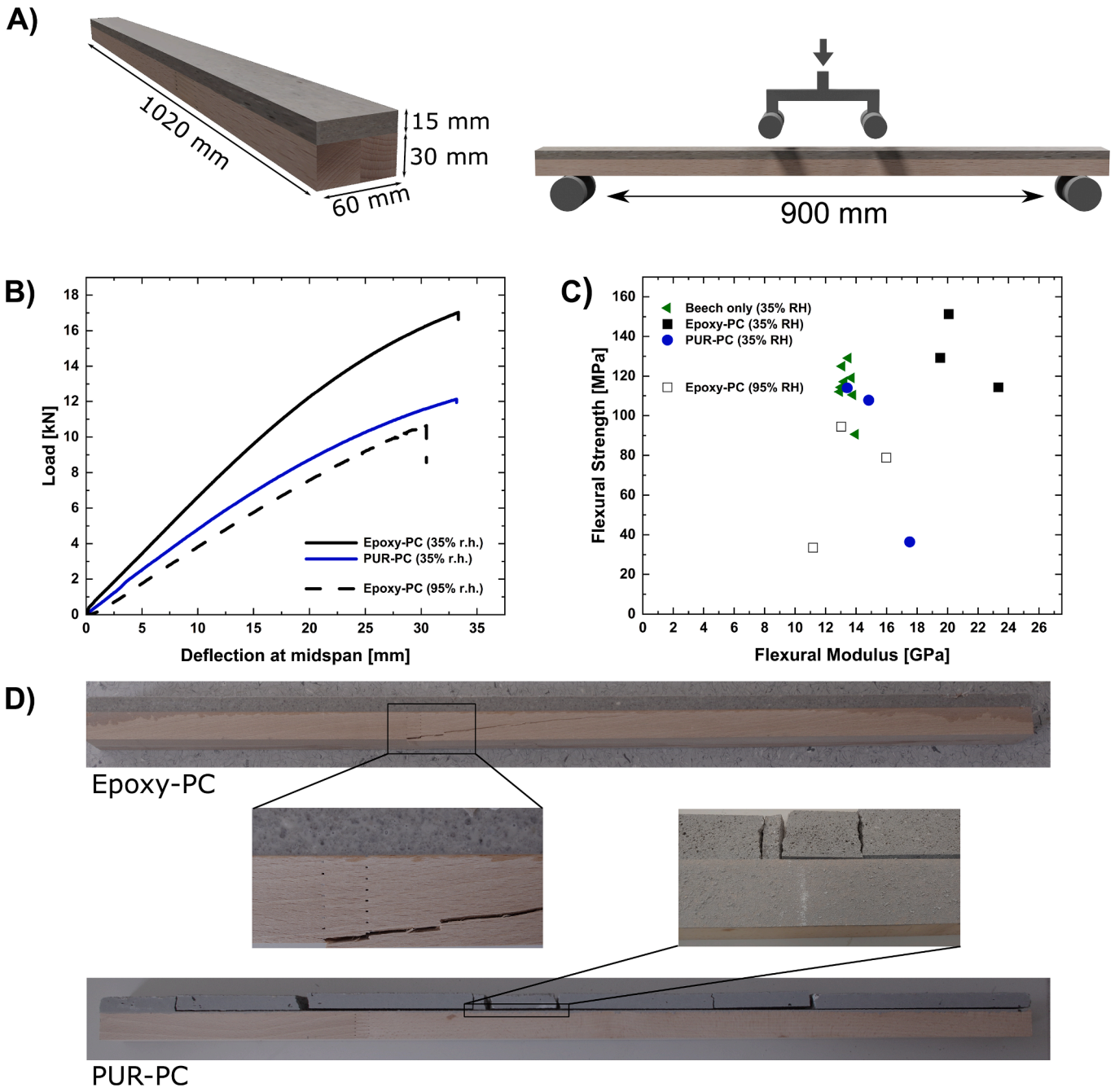


**Fig. 5.** Four-Point Flexural tests of TCCs containing beech in combination with epoxy- and PUR- PC. A) Scheme of the sample geometry and dimensions and four-point bending test setup. B) A typical force–deflection curve of the sample in dry state (35 % RH) and after storage at 95 % RH. C) Flexural strength and stiffness of TCC beams with different PC and moisture contents. D) Typical fracture pattern of the TCC beams in dry state with epoxy-PC (top) and PUR-PC (bottom).

### *3.4.3. Influence of moisture on flexural performance*

Since a strong influence of moisture on the bond strength has been observed in the shear test samples, additional flexural tests were conducted after conditioning the beams at a high humidity of 95 % RH. Such high wood moisture levels (WMC ≈ 22 %) resulted in a decrease in stiffness of the TCC with epoxy-PC with an average flexural stiffness of 13.6 ± 0.3 GPa (Fig. 5). Out of the three tested beams, two showed flexural tensile failure, while only one specimen failed in shear at the interface. The different failure modes were also reflected in the flexural strength, as the latter specimen showed an obviously lower strength of 34 MPa compared to 95 and 79 MPa, respectively. TCCs with PUR-PC delaminated during storage at high humidity of 95 % RH due to the swelling of the wood and were not tested. However, the failure was in accordance with the observations made for shear samples and occurred as a near interface cohesion failure.

### *3.5. Effect of the PC matrix on the deformation behaviour of millimeter-scale TCCs under moisture influence*

The influence of moisture became obvious in the mechanical tests. Both, TCC with epoxy- and PUR-PC showed a decrease in bond strength after exposure to moisture. However, specimens with PUR-PC exhibited generally lower strengths and moisture resistance than epoxy-PC bonded samples. The results indicate that not the adhesion strength of the respective resin to the beech wood determines the bond strength, but rather the strength of the concrete, specifically in the region close to the

**Table 3**
Summary of the maximal force $F_{max}$ and deflection $w_{max}$ at the point of failure of the TCC beams in dry state. The governing strengths of the subcomponents where the failure occurred are written in bold.

| | Epoxy-PC Specimen | | | PUR-PC Specimen | | |
|---|---|---|---|---|---|---|
| | 1 | 2 | 3 | 1 | 2 | 3 |
| Finger joint[a)] | no | yes (160 mm) | yes (190 mm) | no | yes (0 mm) | no |
| Fracture mode | flexural-tension | flexural-tension | flexural-tension | shear | shear | shear |
| $F_{max}$ [kN] | 17.03 | 12.87 | 14.54 | 12.11 | 4.10 | 12.84 |
| $w_{max}$ [mm] [b)] | 35.21 | 19.86 | 28.6 | 29.65 | 8.02 | 35.67 |
| $f_{v,G}$ [MPa] [c)] | 4.62 | 3.49 | 3.94 | **3.28** | **1.11** | **3.48** |
| $f_{tm,w}$ [MPa] [c)] | **127.74** | **96.50** | **109.06** | 92.41 | 31.30 | 98.00 |
| $f_{c,B}$ [MPa] [c)] | 186.45 | 140.85 | 159.18 | 137.35 | 46.52 | 145.66 |

a) Indicates if a finger joint was present in the specimen. The distance of the finger joint to the centre of the beam is noted in brackets.
b) Midspan deflection w at maximal load $F_{max}$.
c) Shear stress $f_{v,G}$ acting at the bondline, compression stress $f_{c,B}$ in the concrete and bending tensile stress $f_{tm,w}$ in the timber at the moment of fracture.

bondline.

To characterize the behaviour of the TCC during the moisture-induced swelling in more detail, we developed a simple experimental setup to in situ monitor the strains developed across the bondline of the composite. Complementary to the mechanical testing of TCC, which showed the holistic mechanical behaviour, we employed DIC to monitor moisture-induced local surface deformations in the vicinity of the bondline as shown in Fig. 6. For this purpose, millimeter-scale TCC samples were prepared, fully cured and conditioned in a dry climate (35 % RH). After the application of a speckle pattern, the samples were exposed to high humidity (≈ 90 % RH) for several days, while being in situ monitored until no additional dimensional changes were observed. The resulting Lagrangian strains of samples with epoxy- and PUR-PC after swelling of the wood are visualized in Fig. 6B and 6C. The measured strains reflect the deformations measured on the surface of the specimens. Even though out-of-plane deformations are minimized by observing the cross-section of the specimens, border effects cannot be fully ruled out.

The two PC matrices showed different behaviour upon deformation imposed by the wood swelling. The epoxy-PC did not deform in the matrix, with strain developed exclusively in the wood. The PC stabilized the interface and restricted the swelling of the wood. This led to a gradual increase in swelling strain starting from the interface, with the maximum swelling strain of the wood being reached several millimeters away from the bondline (Fig. 6D). Such behaviour was proposed by Frazier [42] to occur in highly moisture-stable, in-situ polymerized wood adhesives (e.g. phenol–formaldehyde adhesives), where the gradual transfer of the swelling strain into the wood reduces stress concentrations on the bondline and increases the moisture resistance of the bond. The effective stress levels acting on the bondline cannot be directly quantified with the DIC measurement [44]. Nonetheless, the gradual distribution of the strain away from the bondline into the wood indicates limited shear stress concentrations at the bondline, as seen by the shear strain $\varepsilon_{xy}$ in Fig. 6B.

In contrast, the PUR-PC specimens showed deformations in the vicinity of the bondline. Two out of eight specimens restricted the wood swelling and exhibited a deformation behaviour similar to epoxy-PC with a stabilization of the wood interface, but for the majority of the specimens, less stabilization of the wood surface occurred. The swelling of the wood imparted high shear strains (and consequently stresses) on the concrete, which led to the failure of the PC upon reaching its fracture strain. This behaviour is in accordance with the near interface cohesion failure observed in the TCC with PUR-PC tested in shear and bending.

The different deformation mechanisms of the TCCs which result from the swelling of the wood cannot be simply explained by the elastic properties of the concrete, as both of the resins have a similar elastic modulus (2.9 and 3.3 GPa for PUR- and epoxy-resin, respectively). The different behaviour of the TCCs with PUR-PC is presumably due to crack formation near the interface in the PC. The formation of cracks relaxes the restricting forces at the interface and allows the swelling of wood, without complete failure of the specimen though. As seen in Fig. 6C, the strain fields obtained by DIC suggest the occurrence of subsurface cracks starting from the bondline into the PUR-PC, which shows visible crack propagation in the bulk with increased strains. A similar effect has previously been shown by Ren and Hu [45] during investigations on the fatigue behaviour of epoxy-PC and PUR-PC under cyclic loading. They observed increased deformations and reduced stiffness modulus with increasing stress levels, presumably due to crack formation at the surface and internal defects.

The comparison of strain fields visualized by a false colour map can be misleading, especially in case of minor differences in strains or due to the occurrence of inhomogeneous strains, as often seen in wood samples. To facilitate quantification and comparison of the strains which developed perpendicular to the bondline, a sub-selection of the obtained 2D-strain field was chosen (excluding regions with obvious border effects, defects in the sample or defects from the DIC analysis) and reduced to a 1-D deformation curve by averaging the horizontal strains ($\varepsilon_{xx}$). Fig. 6D and 6E show the strain in the TCC that developed after increasing the humidity, with and without pre-treatment of the wood with an adhesion primer. It can be seen that even though cracks are formed in the PUR-PC, a certain amount of adhesion is still present. This leads to a deformation of the PUR caused by swelling the wood and results in a structurally weakened interface due to the partial failure of the PUR-PC. It is also visible that pre-treatment of the wood surface with an adhesion primer influenced the swelling behaviour only marginally.

The different behaviour of the two PC is presumably dictated by the inherent lower strength of the PUR-PC than the epoxy-PC. An additional reason that may partially contribute is assumed to be the formation of an interface-near region with reduced strength due to the reaction of the PUR-PC with moisture from the wood surface. In Fig. 2B, it can be seen that $T_g$ at the interface differs from the bulk of the PUR-PC. This indicates a reaction with wood components, most likely water, that generates gaseous $CO_2$, which has not only the potential to weaken the interface by trapped gas bubbles but also to influence the crosslinking density and thus the mechanical properties of the PUR-PC [41,46]. The properties of this interfacial region can partially be influenced by the application of an adhesion primer. However, the effect of the primer on the bond shear strength is not pronounced and can only be observed in dry state of the sample. After exposure to moisture, the swelling forces still mostly lead to failure of the PUR-PC and no effect of the adhesion primer on the moisture resistance can be observed.

## 4. Conclusion

TCCs with epoxy-PC showed higher strength and better short-term moisture stability than TCCs with PUR-PC. The behaviour of the TCCs with epoxy-PC under the influence of moisture showed, that even with beech and its low dimensional stability, it is possible to obtain a rather stable bond to the concrete after exposure to water. PUR-PC was not able to withstand the swelling of the wood and fractured often as a near

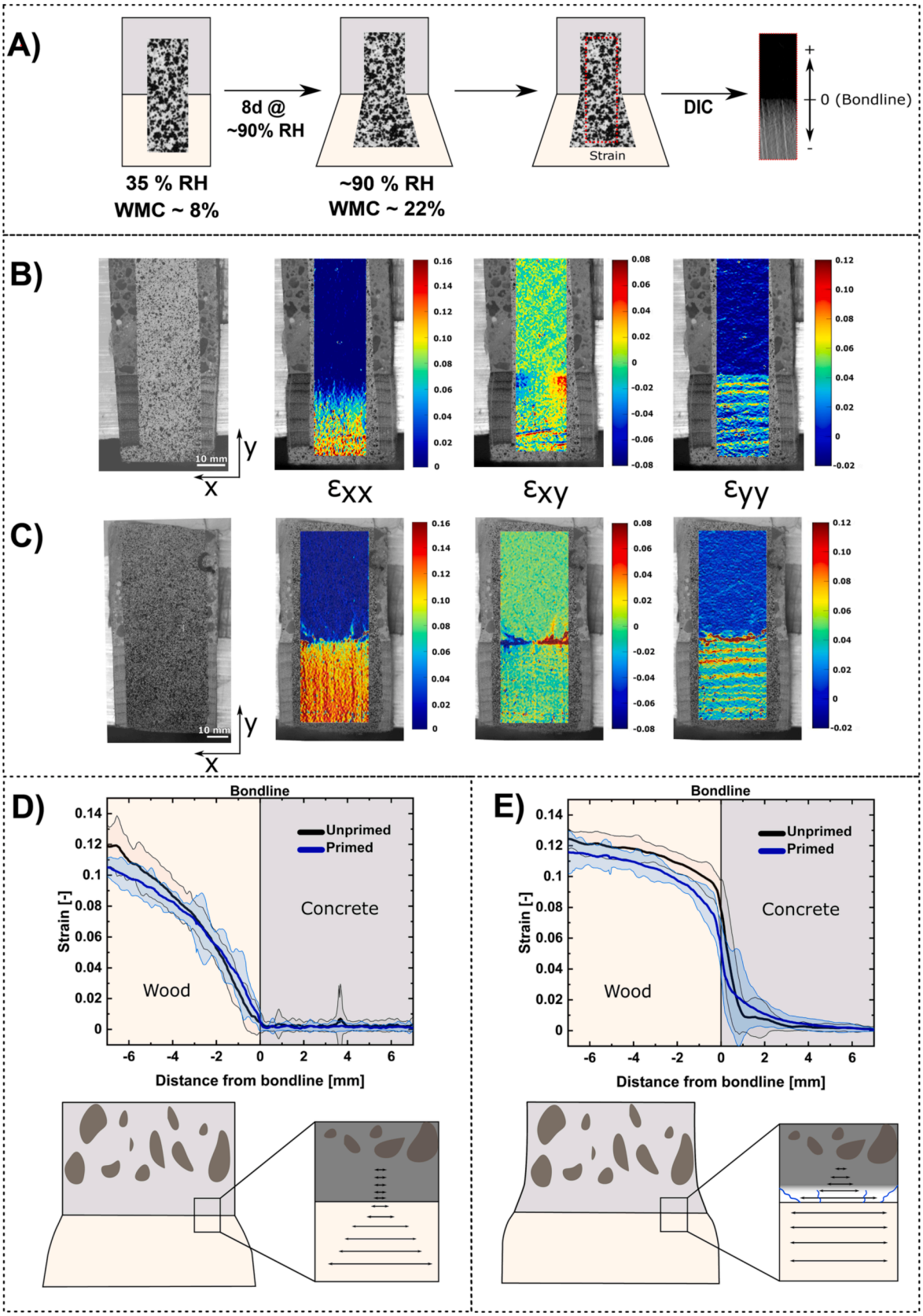


**Fig. 6.** DIC-measurement of the deformation behaviour of the TCC. A) Experimental setup. The 2D-strain fields (εxx, εxy, εyy) after the moisture induced-swelling are shown in B) for epoxy-PC and C) PUR-PC. 1D strain curve (εxx) for the D) epoxy-PC and E) PUR-PC. The arrows indicate the observed strain schematically and are not drawn to scale.

interface cohesion failure.

An in-depth investigation of the swelling effect using DIC showed that TCCs with the two PC deform very differently, with the epoxy-PC restricting the wood swelling. In contrast, in TCCs made with PUR-PC, beech wood swelling was only minimally restricted due to crack formation in the PC near the interface. The investigation of the swelling behaviour showed that even when TCCs are designed in a way that applied loads should only lead to compression stresses in the concrete and shear stresses at the bondline, the moisture-induced swelling strain of the beech wood can generate additional tensile and shear forces in the PC. Thus, for TCCs with beech wood, the tensile strength of the PC plays an important role to achieve a reliable and moisture-resistant composite, which should be taken into consideration for the further development of moisture-resistant TCCs with PCs.

PCs, and in particular epoxy-PC, could be viable replacements for cement-based concretes for application in TCC. The self-adhesion of the concrete to the wood allows for facilitated manufacturing of such composites, and the excellent tensile and compression strengths of polymer concrete in combination with beech wood would allow to realize lightweight TCC structures with reduced layer thickness, while maintaining comparable load-carrying capability to commonly used OPC concrete based TCCs.

## CRediT authorship contribution statement

**Sandro Stucki:** Writing – original draft, Methodology, Investigation. **Steffen Kelch:** Writing – review & editing, Methodology, Conceptualization. **Tim Mamie:** Methodology, Investigation. **Urs Burckhardt:** Writing – review & editing, Conceptualization. **Philippe Grönquist:** Writing – review & editing, Methodology. **Roman Elsener:** Investigation. **Mark Schubert:** Supervision, Writing – review & editing. **Andrea Frangi:** Writing – review & editing, Funding acquisition, Conceptualization. **Ingo Burgert:** Conceptualization, Supervision, Funding acquisition, Writing – review & editing.

## Declaration of Competing Interest

Urs Burckhardt, Steffen Kelch, Tim Mamie, Ingo Burgert, Andrea Frangi, Philippe Grönquist and Sandro Stucki have the patent: “Method for producing a laminate from wood and a curable composition (WO 2023/148056 A1″ issued to Sika Technology AG and EMPA Eidgenössische Materialprüfungs- und Forschungsanstalt.

## Data availability

Data will be made available on request.

## Acknowledgements

We sincerely thank the Swiss Innovation Agency Innosuisse for financial support of the project (Project. No. 37233.1 IP-ENG “ Adhesive-bonded timber-concrete composites – Using beech wood and polymer concrete for innovative solutions”). Furthermore, we are grateful to Fagus Suisse SA for providing the beech wood. We appreciate support in the design and carrying out of experiments by Martin Arnold, Daniel Heer and Walter Risi.

## Appendix A. Supplementary data

Supplementary data to this article can be found online at https://doi.org/10.1016/j.conbuildmat.2023.134069.

## References

[1] D. Yeoh, M. Fragiacomo, M. De Franceschi, B.K. Heng, State of the art on timber-concrete composite structures: literature review, J. Struct. Eng. 137 (2011) 1085–1095.
[2] L. Eisenhut, W. Seim, S. Kühlborn, Adhesive-bonded timber-concrete composites – Experimental and numerical investigation of hygrothermal effects, Eng. Struct. 125 (2016) 167–178.
[3] Q. Fu, L. Yan, N.A. Thielker, B. Kasal, Effects of concrete type, concrete surface conditions and wood species on interfacial properties of adhesively-bonded timber - concrete composite joints, Int. J. Adhes. Adhes. 107 (2021) 102859–102868.
[4] M. Kästner, K. Rautenstrauch, Polymermörtel-Klebverbindungen für Holz-Beton-Verbundbrücken Teil 1, Bautechnik 98 (2021) 23–30.
[5] S. Kostić, V. Merk, J.K. Berg, P. Hass, I. Burgert, E. Cabane, Timber-mortar composites: The effect of sol-gel surface modification on the wood-adhesive interface, Compos. Struct. 201 (2018) 828–833.
[6] J.H.J.O. Negrao, C. Oliveira, F.M.M. Oliveira, Investigation on Timber-concrete glued composites. 9th World Conference on Timber Engineering (9 WCTE). Portland, U.S.A.2006.
[7] A. Nemati Giv, Q. Fu, L. Yan, B. Kasal, Interfacial bond strength of epoxy and PUR adhesively bonded timber-concrete composite joints manufactured in dry and wet processes, Constr. Build. Mater. 311 (2021) 125356–125372.
[8] M. Schäfers, W. Seim, Investigation on bonding between timber and ultra-high performance concrete (UHPC), Constr. Build. Mater. 25 (2011) 3078–3088.
[9] K.-U. Schober, Untersuchungen zum Tragverhalten hybrider Verbundkonstruktionen aus Polymerbeton, faserverstärkten Kunststoffen und Holz [Dissertation], Bauhaus-Universität Weimar, Weimar, Germany, 2008.
[10] T. Tannert, B. Endacott, M. Brunner, T. Vallée, Long-term performance of adhesively bonded timber-concrete composites, Int. J. Adhes. Adhes. 72 (2017) 51–61.
[11] M. Brunner, M. Romer, M. Schnüriger, Timber-concrete-composite with an adhesive connector (wet on wet process), Mater. Struct. 40 (2007) 119–126.
[12] J. Frohnmüller, J. Fischer, W. Seim, Full-scale testing of adhesively bonded timber-concrete composite beams, Mater. Struct. 54 (2021) 187–208.
[13] J. Frohnmüller , W. Seim , M. Mérono , G. Wisner , E.Stammen, Adhesively bonded Timber-Concrete Composites with Smooth Concrete Surfaces. World Conference on Timber Engineering (WCTE). Santiago, Chile2021.
[14] S. Arendt, M. Sutter, M. Breidenbach, R. Schlag, V. Schmid, Neue Forschungsergebnisse zu Nass-in-Nass geklebten Holz-Beton-Verbunddecken, Bautechnik 99 (2022) 56–65.
[15] K-U. Schober, Strengthening of timber floors with concrete-type adhesives, Proceedings of the Institution of Civil Engineers - Structures and Buildings 173 (2020) 320–325.
[16] J. Kanocz, V. Bajzecerova, Timber-concrete composite elements with various composite connections part 3: adhesive connection, Wood Res. 60 (2015) 939–952.
[17] A. Nemati Giv, Z. Chen, Q. Fu, T. Leusmann, L. Yan, D. Lowke, et al., Bending behavior and bond analysis on adhesively bonded glulam-concrete panels fabricated with wet bonding technique, J. Build. Eng. 76 (2023) 107140–107156.
[18] M. Füchslin , P. Grönquist ,S. Stucki , T. Mamie , S. Kelch , I. Burgert , et al. Push-out tests of wet-process adhesive-bonded beech timber-concrete and timber-polymer-concrete composite connections. World Conference on Timber Engineering (WTC) 2023. Oslo, Norway2023.
[19] O. Figovsky, D. Beilin, Advanced Polymer Concretes and Compounds, 1st ed., CRC Press, Boca Raton, 2013.
[20] M.M. Reda Taha, M. Genedy, Y. Ohama, 17 - Polymer concrete, in: S. Mindess (Ed.), Developments in the Formulation and Reinforcement of Concrete (second Edition), Woodhead Publishing, 2019, pp. 391–408.
[21] K. Erler, Verstärkung von Holzbalkendecken mit Polymerbeton, in: G. König, K. Holschemacher, F. Dehn (Eds.), Holz-Beton-Verbund: Innovationen Im Bauwesen : Beiträge Aus Praxis Und Wissenschaft Berlin, Bauwerk Verlag, Berlin, 2004.
[22] K. Korhonen, S. Göran, A. Freudenschuss, U.-B. Brändli, J. Fridman, E. Cienciala, et al., Criterion 1: Maintenance and appropriate enhancement of forest resources and their contribution to global carbon cycles. FOREST EUROPE: State of Europe’s Forests 2020: Ministerial Conference on the Protection of Forests in Europe, 2020.
[23] R. Wagenführ, A. Wagenführ, Holzatlas, 7 ed., Carl Hanser Verlag, München, 2021.
[24] A.W. Christiansen, C.B. Vick, E.A.A. Okkonen, Novolak-Based Hydroxymethylated Resorcinol Coupling Agent for Wood Bonding. Wood Adhesives. South Lake Tahoe, Forest Product Society, Nevada, USA, 2001.
[25] C.B. Vick, K. Oksman, Durability of one-part polyurethane bonds to wood improved by HMR coupling agent, For. Prod. J. 50 (2000) 69–75.
[26] S. Kostić, S. Meier, E. Cabane, I. Burgert, Enhancing the performance of beech-timber concrete hybrids by a wood surface pre-treatment using sol-gel chemistry, Heliyon 4 (2018) e00762.
[27] Fagus Suisse SA. Fagus Stabschichtholz - Bemessungswerte für Buche. 2023.
[28] DIN EN ISO 11357-2. Plastics – Differential scanning calorimetry (DSC) – Part 2: Determination of glass transition temperature and step height. Berlin: Beuth Verlag GmbH; 2020.
[29] DIN EN ISO 527-3:2019-02. Plastics - Determination of tensile properties - Part 3: Test conditions for films and sheets (ISO 527-3:2018); German version EN ISO 527-3:2018. Berlin: Beuth Verlag GmbH; 2019.
[30] P. Grönquist , M. Füchslin , S. Gianinazzi , A. Albertini , S. Stucki , I. Burgert , et al. Tragverhalten von verklebten Holz-Beton- und Holz-Polymerbeton-Verbunddecken mit Buchen-Stabschichtholz. S-WIN-Tagung 2022: Von der Forschung zur Praxis: Sicher mit Holz. Online: S-WIN Swiss Wood Innovation Network; 2022.

[31] 527-1:2019-12: DEI. Plastics – Determination of tensile properties – Part 1: General principles (ISO 527-1:2019); Berlin: Beuth Verlag GmbH; 2019.
[32] DIN 52 186. Testing of Wood: Bending Test, Beuth Verlag GmbH, Berlin, 1978.
[33] DIN EN 1995-1-1:2010-12. Eurocode 5: Design of timber structures — Part 1-1: General — Common rules and rules for buildings. Berlin: Beuth Verlag; 2004.
[34] The MathWorks Inc. Matlab Computer Vision Toolbox. R2020b ed. Natick, Massachusetts, United States: The MathWorks Inc.; 2022.
[35] J. Schindelin, I. Arganda-Carreras, E. Frise, V. Kaynig, M. Longair, T. Pietzsch, et al., Fiji: an open-source platform for biological-image analysis, Nat. Methods 9 (2012) 676–682.
[36] S. Bossuyt, Optimized patterns for digital image correlation, in: H. Jin, C. Sciammarella, C. Furlong, S. Yoshida (Eds.), Imaging Methods for Novel Materials and Challenging Applications, Springer, New York, NY, 2012, pp. 239–248.
[37] J. Blaber, B. Adair, A. Antoniou, Ncorr: Open-Source 2D Digital Image Correlation Matlab Software, Exp. Mech. 55 (2015) 1105–1122.
[38] C.R. Frihart, Wood adhesion and adhesives, in: R.M. Rowell (Ed.), Handbook of Wood Chemistry and Wood Composites, CRC Press, New York, USA, 2005, pp. 215–278.
[39] B. Collett, A review of surface and interfacial adhesion in wood science and related fields, Wood Sci. Technol. 6 (1972) 1–42.
[40] S. Bockel, S. Harling, J. Konnerth, P. Niemz, G. Weiland, E. Hogger, et al., Modifying elastic modulus of two-component polyurethane adhesive for structural hardwood bonding, J. Wood Sci. 66 (2020).
[41] M. Dunky, P. Niemz, Holzwerkstoffe und Leime: Technologie und Einflussfaktoren, Springer-Verlag, Heidelberg, 2013.
[42] C. Frazier, Isocyanate Wood Binders, in: A Pizzi, KL Mittal (Eds.), Handbook of Adhesive Technology, Revised and Expanded, 2nd Edition ed, CRC Press, Boca Raton, 2003.
[43] T. Ehrhart, R. Steiger, M. Lehmann, A. Frangi, European beech (Fagus sylvatica L.) glued laminated timber: lamination strength grading, production and mechanical properties, Eur. J. Wood Wood Prod. 78 (2020) 971–984.
[44] K. Markus, P. Niemz, J.-W. van de Kuilen, Measurement of moisture-related strain in bonded ash depending on adhesive type and glueline thickness, Holzforschung 70 (2016) 145–155.
[45] S. Ren, X. Hu, Fatigue properties and its prediction of polymer concrete for the repair of asphalt pavements, Polymers 14 (2022) 2941–2954.
[46] P. Bliem, H.W.G. van Herwijnen, M. Riegler, J. Konnerth, Investigation of important influencing factors on the tensile shear strength of two component polyurethane with distinct foaming behaviour, Int. J. Adhes. Adhes. 84 (2018) 343–349.